CONTRIBUTIONS TO THE STABILITY ANALYSIS OF EXPLICIT ENRICHED MESHFREE METHODS

Esteban Samaniego[a], Hossein Talebi[b], Cristóbal Samaniego[c] and Timon Rabczuk[b]

[a]*Civil Engineering School, Facultad de Ingeniería, Universidad de Cuenca, Av. 12 de Abril s/n., Cuenca, Ecuador; email: esteban.samaniego@ucuenca.edu.ec*

[b]*Institute of Structural Mechanics, Bauhaus–Universitat Weimar, Marienstrasse 15, D-99423 Weimar, Germany; email:timon.rabczuk@uni-weimar.de*

[c]*Computer Applications in Science and Enginnering Department, Barcelona Supercomputing Center (BSC-CNS), Edificio Nexus I, Campus Nord UPC Gran Capitán 2-4, Barcelona Spain; email: cristobal.samaniego@bsc.es*

Keywords: Meshfree methods, explicit integration, critical time step, lumped matrix.

Abstract. Meshfree methods have certain advantages with respect to other more classical numerical methods. The Element Free Galerkin Method (EFGM), in particular, seems to offer a good performance when dealing with problems that include the treatment of large deformations together with the presence of strong or weak discontinuities to model cracks or material interfaces. A possible approach is to introduce the discontinuity to the discretization by adding special enrichment functions to the standard shape functions. The cracking particles method, based on EFGM, is an example of such approaches. When dealing with dynamic applications by means of explicit time integration schemes, a lumped mass matrix is necessary for an efficient numerical simulation. However, when the shape functions include discontinuous enrichment, studying the behavior of the critical time step becomes problematic. Moreover, it may tend to very small values, thus leading to computationally expensive simulations. In this work, we present some contributions to the study of these stability issues for an explicit enriched EFGM for one- and two-dimensional problems.

1 INTRODUCTION

Meshfree methods posses some advantages over the widely used finite element method when the material undergoes large deformation and fracture. One of these advantages is the possibility of enriching the standard shape functions in a very natural way. Within the finite elements context, the so-called Extended Finite Elements (XFEM), which was introduced by Belytschko and his group in Belytschko and Black (1999); Moes et al. (1999); Dolbow et al. (2000), is based on the so-called partition of unity methods (PUM) Babuška and Melenk (1997). In XFEM, the representation of a strong or weak discontinuity is done via enrichment of the shape functions. Therefore the crack representation as, for example, a strong discontinuity within the element edges or remeshing is no longer needed. The concept of discontinuity enrichment has been used in the EFG method and successfully applied for static and dynamic problems Ventura et al. (2002); Rabczuk and Belytschko (2004, 2006); Rabczuk et al. (2007).

In dynamic problems, mass lumping is commonly used in order to avoid solving a system of equations. However, when XFEM is used for dynamic crack propagation, the extra degrees of freedom and the enriched shape function introduce some unusual behavior in the mass matrix. Belytschko et al. (2003) were the first to point out the possibility of a very small critical time step for X-FEM.

Menouillard et al. (2008, 2006) have addressed the problem and offered a strategy for mass lumping when the approximation spaces are enriched. This strategy prevents the critical time step to vanish and it is in the order of the critical time step for the model without cracks. In Talebi et al. (2010), this framework is extended by the authors in order to apply it to meshless methods. The high sensitivity of the critical time step to the relative crack location and the nodes is dealt with in this reference. However, there is no straightforward way of building a diagonalized mass matrix for extended meshfree method. Thus, we first must briefly examine the critical time step for the consistent mass matrix for extended meshfree. Then, two strategies for mass lumping for one and two dimensional problems are presented. Once this is done, we can analyze the critical time step with the proposed lumping strategies and show that the order of critical time step for the new lumped mass matrices is the same as the one without a discontinuity.

The remaining of this paper is organized as follows. In Section 2, we write the governing equations. Section 3 deals with the EFG and enriching meshfree shape functions. Next, the general mass lumping formulas are derived and applied to crack modeling. Critical time steps estimates are introduced. Some issues about the stability of the resulting formulations are tackled by means of a combination of numerical experiments and analytical estimates. Finally, some conclusions are extracted.

2 GOVERNING EQUATIONS

Consider a domain Ω in R^D, corresponding to the current position of a solid, with boundary Γ, where D is the dimension of the physical space (in this paper $D = 2$ unless stated otherwise). The images of Ω and Γ in the initial configuration are the Ω_0 and Γ_0, respectively. By choosing the reference state as the initial state, the strong form of linear momentum equation in total Langrangian description is

$$\nabla_0 \cdot \boldsymbol{P} + \varrho_0 \boldsymbol{b} = \varrho_0 \ddot{\boldsymbol{u}} \qquad \text{in } \Omega_0 \backslash \Gamma_0^c \tag{1}$$

and the boundary conditions are

$$n_0 \cdot P = \bar{t}_0 \qquad \text{on } \Gamma_0^t \tag{2}$$

$$u = \bar{u} \quad \text{on } \Gamma_0^u \tag{3}$$

$$n_0^C \cdot P^- = n_0^C \cdot P^+ = t_{c0} \quad \text{on } \Gamma_0^c \tag{4}$$

where P is the nominal stress, ϱ_0 is the initial density, b are the body forces, u and $\ddot{u}$ are the displacements and accelerations, respectively; n_0 is the normal to the boundary in the initial configuration, $\bar{u}$ and $\bar{t}$ denote the prescribed displacements and traction, respectively, considering that the structure is subjected to a set of displacement and traction boundary conditions on the disjoint complementary parts of the boundary in the initial configuration, i.e. Γ_0^u and Γ_0^t; P^- and P^+ denote the nominal stress at the left and at the right of the discontinuity, respectively, n_0^C is the normal to the discontinuity, and t_{c0} is the traction on the interface.

3 EXTENDED ELEMENT FREE GALERKIN METHOD(XEFG)

Meshfree approximations in terms of the material (Lagrangian) coordinates can be written as

$$u^h(X, t) = \sum_{I \in \mathcal{W}} \Phi_I(X) u_I(t) \tag{5}$$

where $\Phi_I(X)$ are the shape functions and u_I is the value at the particle parameter (it is, usually, nearly equal to the displacement) at the position X_I, and $\mathcal{W}$ is the set of particles for which $\Phi_I(X_J) \neq 0$. Note that the above form is identical to the form of an FEM approximation. However, in contrast to FEM, $\Phi_I(X)$ is only an approximant and not an interpolant, since $u(X_I) \neq u_I$. Therefore special techniques are needed to treat displacement boundary conditions; see for example Fernandez-Mendez and Huerta (2004).

In the EFG method the shape function Φ is defined as

$$\Phi_I = p(X)^T \cdot A(X)^{-1} \cdot p_I(X) W(X - X_I, h), \tag{6}$$

$$A(X) = \sum_{I \in S} p_I(X) p_I^T(X) W(X - X_I, h). \tag{7}$$

where p is the basis function and h is the dilation parameter which are explained in Belytschko et al. (1994) in detail. In addition to the fact that the order of continuity can be increased quite easily, meshfree methods have advantages over finite elements because of their smoothness and nonlocal interpolation character. Moreover, better stress distributions around the crack tip are obtained, promising a less oscillatory crack path.

Representation of the crack in the XEFG method is realized via enriching the test and trial functions with additional unknowns so that the approximation is continuous in the whole domain but discontinuous along the crack as done in many former methods such as XFEM Moes et al. (1999). The approximation is:

$$u^h(X) = \sum_{I \in \mathcal{W}} \Phi_I(X) u_I + \sum_{I \in \mathcal{W}_b} \Phi_I(X) H(f_I(X)) a_I + \sum_{I \in \mathcal{W}_s} \Phi_I(X) \sum_K B_K b_{KI} \tag{8}$$
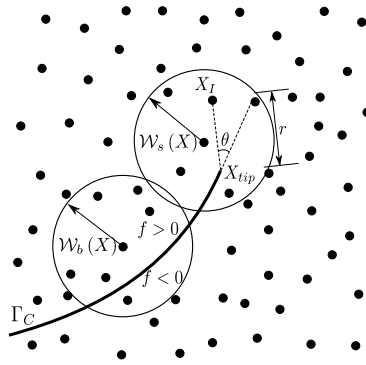
Figure 1: Crack with complete and partial cut domain of influence nodes

where $\mathcal{W}(\boldsymbol{X})$ is the entire domain, $\mathcal{W}_b(\boldsymbol{X})$ is the completely cut domain, $\mathcal{W}_s(\boldsymbol{X})$ is the partial cut domain, and H and $\boldsymbol{B}$ are the enrichment functions, which are meant to capture the crack tip correctly. The first term on the right hand side of Eq.(8) is the usual approximation, the second and third term are the enrichment, in which the coefficient $\boldsymbol{a}$ and $\boldsymbol{b}$, respectively, are additional unknowns introduced for the crack.

$H(f(\boldsymbol{X}))$ depends on the signed distance function $f_I(\boldsymbol{X})$ and is defined as:

$$H(f(\boldsymbol{X})) = \begin{cases} H(f_I(\boldsymbol{X})) = 1 & if \ f_I(\boldsymbol{X}) > 0 \\ H(f_I(\boldsymbol{X})) = -1 & if \ f_I(\boldsymbol{X}) < 0 \end{cases} \tag{9}$$

with

$$f_I(X) = \begin{cases} sign\left[\boldsymbol{n} \cdot (\boldsymbol{X}_I - \boldsymbol{X})\right] \min \|\boldsymbol{X}_I - \boldsymbol{X}\|, & for \ \boldsymbol{X}_I \in \mathcal{W}_b \\ \boldsymbol{n} \cdot (\boldsymbol{X}_{tip} - \boldsymbol{X}_I), & for \ \boldsymbol{X}_I \in \mathcal{W}_s \end{cases} \tag{10}$$

where $\boldsymbol{X}_{tip}$ are the coordinates of the crack tip and $\boldsymbol{n}$ is the crack normal. Only nodes which are located in the domain $\mathcal{W}_b(\boldsymbol{X})$ are enriched with the additional unknowns $\boldsymbol{a}$. The second term of Eq.(8) is called the *step* enrichment.

The third term of Eq.(8) is applied around the crack tip $\mathcal{W}_s(\boldsymbol{X})$. In linear elastic fracture mechanics, $\boldsymbol{B}$ is chosen to be continuous in the whole domain $\mathcal{W}_s(\boldsymbol{X})$, but discontinuous at the crack line.

For cohesive cracks, there is no crack tip singularity and the crack opening displacement, which the cohesive traction depends on, may be described by the additional unknown $\boldsymbol{a}$ only. Assuming the equal test and trial functions and after substituting them in the weak form, the final form of the equation of motion is obtained by

$$\mathbf{M}_{IJ} \cdot \ddot{\mathbf{D}}_{\mathbf{I}} = \mathbf{F}_{\mathbf{I}}^{\mathbf{ext}} - \mathbf{F}_{\mathbf{I}}^{\mathbf{int}} \tag{11}$$

where $\mathbf{M}$ is the consistent mass matrix and $\mathbf{F}^{int}$ are the internal forces. The cohesive forces are taken into account in the external forces, $\mathbf{F}^{ext}$. Gauss quadrature is used to obtain the discrete equations. Generally, four nodes are arranged so that they form the quadrature cell. Integration cells that are cut by a crack are sub-triangulated as in XFEM. Please refer to Rabczuk and Zi (2007) for the details of integration technique used here and the derivation of equations.
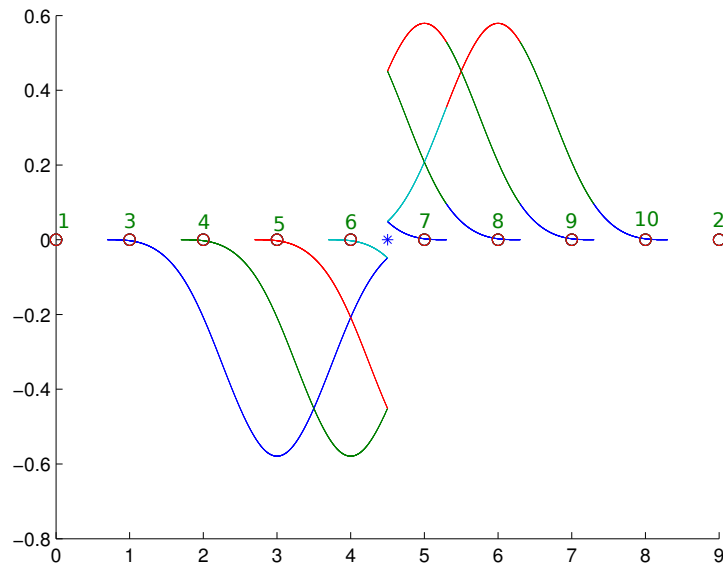
Figure 2: Enriched shape functions for a set of ten nodes with the point of discontinuity at $X_{cr} = 4.5$

4 LUMPED MASS AND THE TIME STEP ESTIMATES

It is well-known that the explicit time integration is conditionally stable and, in order to guarantee stability, the critical time step, Δt_c, should not be exceeded:

$$\Delta t \leq \Delta t_c = \frac{2}{\omega_{max}} \tag{12}$$

where ω_{max} is a solution of the generalized eigenvalue problem $\mathbf{K} - \omega^2 \mathbf{M} = 0$, where $\mathbf{K}$ is the tangent matrix. Thus, $\lambda = \omega^2$ is a generalized eigenvalue.

This classical formula for standard finite elements is presented in textbooks such as Flanagan DP. (1981); Belytschko et al. (2000b). For meshfree methods, the time step estimates without enrichment are presented in Belytschko et al. (2000a); M. A. Puso (2008). According to these references,the lumped mass not only saves us from solving a system of equations but also provides much larger time steps. However the lumping strategy for the mass matrix values of extra degrees of freedom is problematic. Here we analyze the critical time step for the consistent mass matrix of XEFG first and then we propose two methods for the mass lumping of XEFG and show that the critical time step for the new methods is of the order of the critical time step without enrichment through many numerical experiments. We also evaluate the critical time step for various crack positions.

We first start with a 1D bar with patch of 10 particles. The Young's modulus of the bar is $E = 200GPa$ and the density is $7850kg/m^3$. Assume that the domain of influence $(DMAX)$ is 2.3 The particle spacing is uniform and the distance between two neighboring particles is $1m$. The enriched nodes are those whose domain of influence is cut by the crack (point of discontinuity here). Therefore, if for example $DMAX = 2.3$, then the nodes 5,6,7,8 are affected by the crack and therefore should be enriched. Every enriched node will have one extra degree of freedom. Using a step function to model the jump in the displacement field, we build the enriched shape functions that are shown in the Fig.2. The node numbering is also shown in the same figure.

For the step enrichment, H, the consistent mass matrix is calculated by Eq.(11) except that for the 1D case we will not have the branch enrichment $\mathbf{B}$. Using a background cell for integration, at each point of integration the value of the shape functions at the neighboring particles are
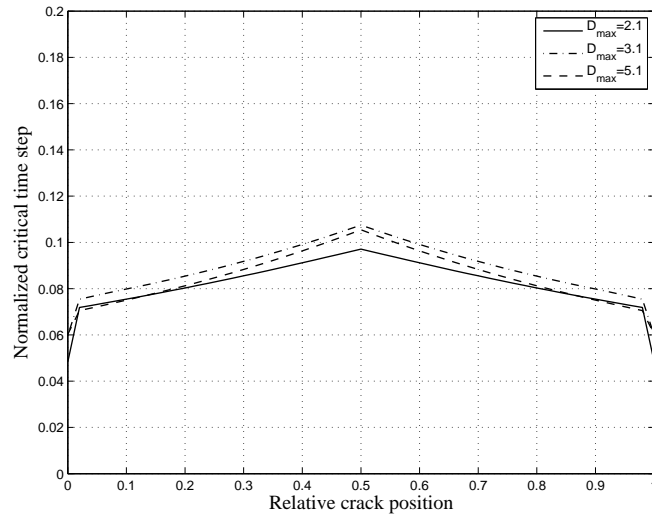
Figure 3: Normalized critical time step versus the crack position for the consistent mass matrix in 1D

calculated and put back to the equation to compute the mass. Thus, the consistent mass matrix for the system in hand and the corresponding extra degrees of freedom is:

$$M = \int_{\Omega_0 \backslash \Gamma_0^c} \varrho_0 \begin{bmatrix} \Phi_1\Phi_1 & \Phi_1\Phi_2 & ... & \Phi_1\Phi_{10} & \Phi_1\tilde{\Phi}_{11} & ... & \Phi_1\tilde{\Phi}_{14} \\ \Phi_2\Phi_1 & \Phi_2\Phi_2 & ... & \Phi_2\Phi_{10} & \Phi_2\tilde{\Phi}_{11} & ... & \Phi_2\tilde{\Phi}_{14} \\ . & & & & & & . \\ . & & & & & & . \\ . & & & & & & . \\ \tilde{\Phi}_{13}\Phi_1 & \tilde{\Phi}_{13}\Phi_2 & ... & \tilde{\Phi}_{13}\Phi_{10} & \tilde{\Phi}_{13}\tilde{\Phi}_{11} & ... & \tilde{\Phi}_{13}\tilde{\Phi}_{14} \\ \tilde{\Phi}_{14}\Phi_1 & \tilde{\Phi}_{14}\Phi_2 & ... & \tilde{\Phi}_{14}\Phi_{10} & \tilde{\Phi}_{14}\tilde{\Phi}_{11} & ... & \tilde{\Phi}_{14}\tilde{\Phi}_{14} \end{bmatrix} d\Omega_0 \quad (13)$$

In the Eq.(13), Φ_I refers to the value of the shape function at the integration point X. For the extra degrees of freedom i.e. 11,12,13,14 here, the value of the shape function is $\tilde{\Phi}_I = \Phi_I H(X - X_{cr})$ and X_{cr} is the position of the crack.

The critical time step, Δt, for the above consistent mass matrix dependens on the position of the crack; however unlike XFEM, due to the smoothed nature of meshfree methods Δt does not vanish when the location of the discontinuity approaches the node (Fig. 3). Moreover Belytschko et al. (2000a) showed that the critical time step depends on the size of domain of influence. Thus, for a patch of nodes with nodal spacing of $1m$ different size of domain of influence($DMAX$), the critical time step versus the relative position of the crack to the neighboring nodes is plotted in the Fig.3 for 1D and Fig.4 for 2D. This shows that, unlike XFEM, a purely explicit approach can be used for dynamic XEFG since the critical time step does not drop to zero. Moreover, the simulation can be run with lumping only the ordinary degrees of freedom and maintaining the consistent mass matrix for the enriched degrees of freedom. Therefore, we only need to solve the system of equations for the enriched degrees of freedom which are few compared to the rest of the system.

4.1 Mass Lumping Strategy 1 (MLS1)

Now we wish to find a full lumped mass matrix which does not have any negative values. As noted in Belytschko et al. (2000a), the ordinary degrees of freedom can be lumped by the row-sum technique. However, for the enriched degrees of freedom the row-sum method is of no
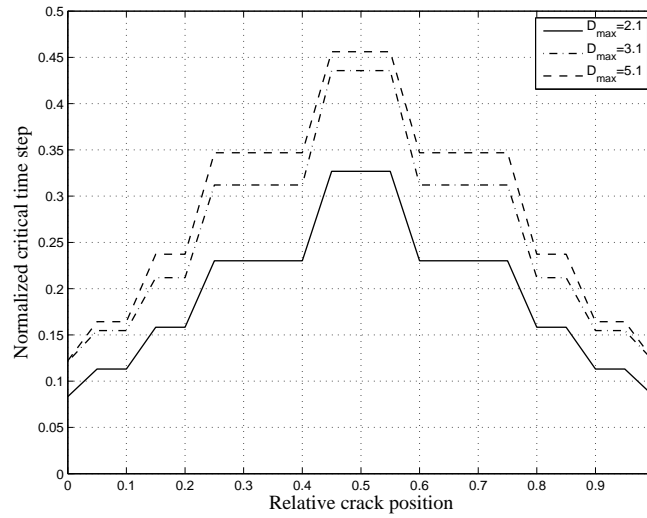
Figure 4: Normalized critical time step versus the crack position for the consistent mass matrix in 2D

use as noted in T. Elguedj (2009) for XFEM. Here we propose to use the special mass lumping technique introduced by Hinton et al. (1976) and also Hughes (1987); Wriggers (2008). This mass lumping strategy always leads to positive masses at the nodes. For finite elements, the idea is to start from a consistent mass matrix and to scale the diagonal terms in such a way that the mass is constant within the element. With little change this procedure can be used for meshfree methods where instead of the elements we have the background cells Li and Liu (2000). Therefore for EFG method we have:

$$m_I^{EFG} = \vartheta_h M_{II} \mathbf{I} \tag{14}$$

where

$$M_{II} = \int_{\Omega_h} \varrho_0 \tilde{\Phi}_I^2 d\Omega \tag{15}$$

and the scaling factor

$$\vartheta_h = \frac{M_h}{\sum_{I=1}^m M_{II}} \qquad , M_h = \int_{\Omega_h} \varrho_0 d\Omega \tag{16}$$

where m is the number of particles that are in the domain of influence of the integration point $\mathbf{X}$ and M_h is the mass of the integration cell. Also, $\tilde{\Phi}_I$ refers to any shape function including enriched and non-enriched ones. Using Eq.(14) leads to a lumped mass matrix that conserves the mass of the whole system even when the enrichment functions exist.

Hinton's special lumping technique retains the diagonal part of the consistent mass matrix, and assumes that the diagonal part of the consistent mass matrix covers the correct frequency range of the dynamic response, whereas the non-diagonal part of the consistent mass matrix is not essential for the final results. This technique ensures the positive definiteness of the mass matrix, and eliminates the singular mode. A possible setback could be that it cuts of the connection, or interaction between the neighboring material particles. However, this setback may be compensated by the non-local nature of mesh-free methods, because each material point in mesh-free methods is covered by more than one shape function; therefore the interaction between the adjacent particles is always present. This lumping technique was proven to produce high-quality, detailed resolution shear-band solutions in numerical simulations using the RKPM Li and Liu (2000).

Figure 5: A sample Gauss point where the neighboring nodes are enriched

4.2　Mass Lumping Strategy 2 (MLS2)

The second lumping strategy is based on the idea proposed by Menouillard et al. (2006); T. Elguedj (2009). The idea is to impose that the discretization preserves the value of the kinetic energy with respect to rigid body translations. Adapting this idea to meshfree methods introduces some complications, mainly due to the fact that, unlike in FEM, the so called Kronecker delta condition is not fulfilled. Thus, we use some simplifying assumptions in order to derive a workable expression for the lumped mass matrix. Numerical experiments will show later the good performance of the obtained expression.

Let us consider an equally spaced sample patch of N nodes, for which there is a point of discontinuity in the middle (see Fig.5). The patch of nodes resembles a finite element or an enriched element when there is a discontinuity. Having this in mind and following Menouillard et al. (2006), we assume that all the nodes in the patch are enriched; therefore we will not consider the blending region. Thus we have N extra degrees of freedom, the same as number of nodes in the patch. As noted in M. A. Puso (2008), for any meshfree or finite element method, the lumped mass of the ordinary degrees of freedom can be calculated by:

$$M_I = \sum_{J=1}^{N} \rho\left(X_J\right) \Phi_I\left(X_J\right) W_J \quad \text{and} \quad M_I = \rho\left(X_I\right) W_I \quad \text{if } \Phi\left(X_J\right) = \delta_{IJ} \tag{17}$$

where W_I is the nodal weighting, which is the length in 1D, the area in 2D and the volume in 3D. Eq.(17) is the same as the result of the row-sum technique to compute the lumped masses. The lumped mass obtained from the expressions at the left and at the right in Eq.(17) are close if the support is tight.

Now we need a mass matrix in the format below:

$$\mathbf{M} = \begin{bmatrix} M_1 & & & & & & \\ & M_2 & & & & 0 & \\ & & \cdot & & & & \\ & & & M_N & & & \\ & & & & M_1' & & \\ & 0 & & & & \cdot & \\ & & & & & & M_N' \end{bmatrix} \tag{18}$$

where M_I are the mass for ordinary degrees of freedom and the M_I' stand for the mass of the extra degrees of freedom. As noted by Menouillard et al. (2006) we can still use the row-sum technique for the usual degrees of freedom. To obtain the mass for the extra degrees of freedom, we use the concept of preserving the value of the exact kinetic energy with respect to rigid body motions. In order to do this, the arbitrary enrichment function ψ is imposed as a constant velocity condition everywhere within the patch of nodes by using the velocity array $\hat{\mathbf{V}} = [\, 0 \quad ... \quad 0 \quad \psi \quad ... \quad \psi \,]^T$, where $\hat{\mathbf{V}}$ denotes the value of the velocity approximation evaluated at the nodes, as opposed to the value of the approximation parameters related to these

nodes, which are arranged in $\mathbf{V}$. Arrays $\hat{\mathbf{V}}$ and $\mathbf{V}$ can be related by the transformation method in Chen and Wang (2000). With the assumptions made above, we can consider that $\hat{\mathbf{V}} = \mathbf{V}$, which, in a general case, does not hold (remember that meshfree shape functions do not satisfy the Kronecker delta properties).

We impose that the corresponding discrete and exact kinetic energies are equal in order to preserve the value of the kinetic energy, which reads

$$\frac{1}{2} \int_\Omega \rho V^2 d\Omega = \frac{1}{2} \mathbf{V}^T \mathbf{M} \mathbf{V} \tag{19}$$

Since the meshfree shape functions we are considering satisfy the partition of unity and velocity is imposed equally to all the additional degrees of freedom, the nodal values of the initial velocity are equal to the real values. Therefore, we will have

$$\frac{1}{2} \int_\Omega \rho V^2 d\Omega = \frac{1}{2} \int_\Omega \psi^2 \rho d\Omega = \frac{1}{2} \mathbf{V}^T \mathbf{M} \mathbf{V} = \frac{1}{2} \hat{\mathbf{V}}^T \hat{\mathbf{M}} \hat{\mathbf{V}} \tag{20}$$

and $\hat{M}_I = \hat{M}_J$, as well as $M_I = \hat{M}_I$. The symbol $\hat{M}_I$ stands for the nodal masses calculated from the shape functions, with $\Phi_I(X_J) = \delta_{IJ}$. Of course, this is not true for the nodes located on the boundary. However, we also assume our patch of nodes is away enough from the boundary. Notice that $\hat{\mathbf{M}}$ and $\mathbf{M}$ are both diagonal and equal to each other, with the assumptions made here. However, in general, we would have to consider a non-diagonal $\mathbf{M}$, which is of no use for our purposes, or $M_I \neq M_J$, which will complicate the expressions of the resulting lumped mass matrix.

With all the above considerations, from Equation (20) we have:

$$\hat{M}_I' = \frac{1}{\sum_{I=1}^{N_Q} \psi^2} \int_\Omega \psi^2 \rho d\Omega \tag{21}$$

This expression is similar to the one obtained in T. Elguedj (2009). Therefore for the step enrichment we obtain:

$$\hat{M}_I' = \frac{1}{\sum_{I=1}^{N} \psi^2} \int_\Omega \psi^2 \rho d\Omega = \frac{1}{\sum_{I=1}^{N} 1^2} \int_\Omega 1^2 \rho d\Omega = \frac{1}{N} \int_\Omega \rho d\Omega = \hat{M}_I \tag{22}$$

4.3 Critical Time Step Analysis

In this section we study the relation between the values of the critical time step for problems with and without cracks. We will show, that the time steps obtained in both cases are similar for the lumping strategies presented in this paper. We then deduce an analytic expression for the critical time step in one dimensional problems without discontinuity, which can also be used for problems presenting a discontinuity. This expression can be generalized for two dimensional problems following a methodology presented in Belytschko et al. (2000a).

Now, we will compare the values of the critical time step obtained with and without cracks for different problems. These values are obtained for both lumping strategies in 1 and 2 dimensions. As mentioned before, the critical time step also depends on the size of the domain of influence ($DMAX$) which is carefully studied. The graphs for the critical time steps are all generated by moving the location of discontinuity from one node to the neighboring node to study how the Δt changes with respect to crack position.
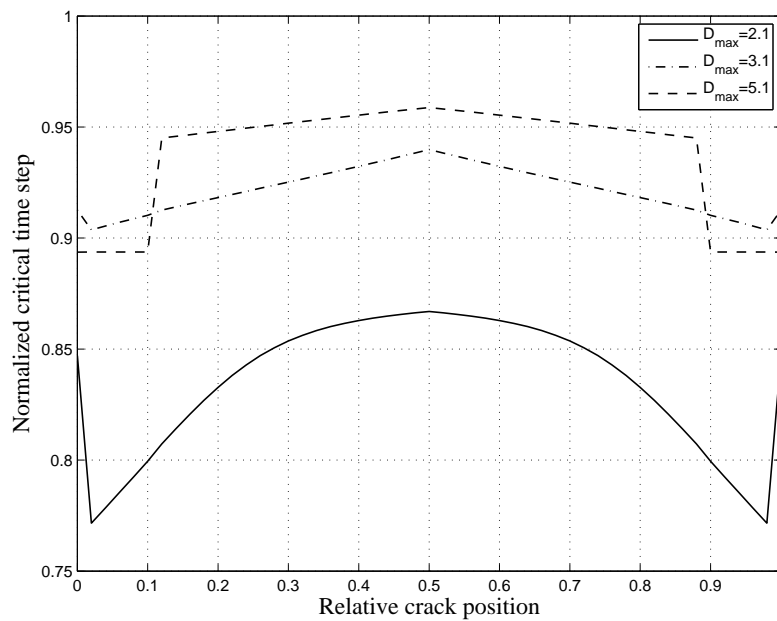
Figure 6: Normalized critical time step versus the crack position for mass lumping strategy 1 (MLS1) in 1D

4.3.1 Critical Time Step for MLS1

We will start with the critical time step results in 1D for the mass lumping strategy 1. Fig.6 shows the normalized Δt for the new lumped mass matrix versus the crack position. As the figure clearly illustrates, Δt_{discon} is of order of Δt_{con}. As can be seen in Fig.6 there is a jump in the graph which belongs to the point that the enriched nodes are changed. This is directly related to the value of $DMAX$. The jumps in the Fig.6 occur due to the change in the nodes to be enriched. In other words when the position of the discontinuity is altered, the enrichment of the nodes changes as well. Fig. 7 also shows the values of Δt versus crack position in 1D. It is obvious that with increasing size of domain of influence(DMAX) the time step size increases; however, a bigger DMAX implies excessive smoothing of the fields and more neighboring nodes which in turn means more computational time.

In 2D, the crack position is varied. We first consider a pure step enrichment, Fig.8, where we vary the crack position in the x direction while the crack completely cuts the patch. Then, the tip is placed at the relative position of $y = 0.9$ and x is varying. This resembles a rather difficult case since the crack tip will be very close to the neighboring nodes. Fig.8 and Fig.10 show the normalized Δt results for mass lumping strategy 1 in 2D with and without tip enrichment. Fig.9 also shows the computed Δt for different DMAX. As it is realized from Fig.10, the order of Δt_{discon} to Δt_{con} for the first lumping strategy drops down to 30 percent.

4.3.2 Critical Time Step for MLS2

Now we will analyze the mass lumping strategy 2 first for pure step enrichment in 1D ,Fig.11. Fig.11 shows the normalized Δt for MLS2 in 1D and Fig.12 shows the computed values of Δt with different DMAX. The critical time step of MLS2(Δt_{discon}.) is similar to Δt_{con}. Similar to the results of MLS1 in 1D, Fig.13, Fig.14, Fig.15 and Fig.16 show the results for Δt in 2D. It can be realized from the figures that the Δt drops to 85 percent which is perfectly usable for explicit dynamic simulations. Moreover, the changes in Δt with respect to DMAX complies with the results obtained by Belytschko et al. (2000a) in the continuous problem. While the
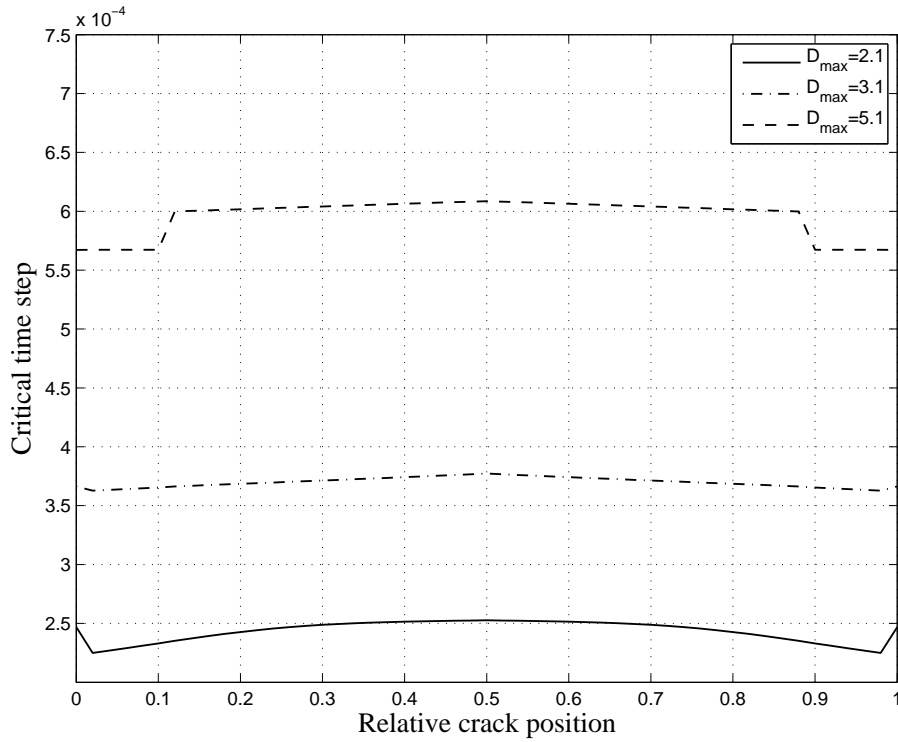
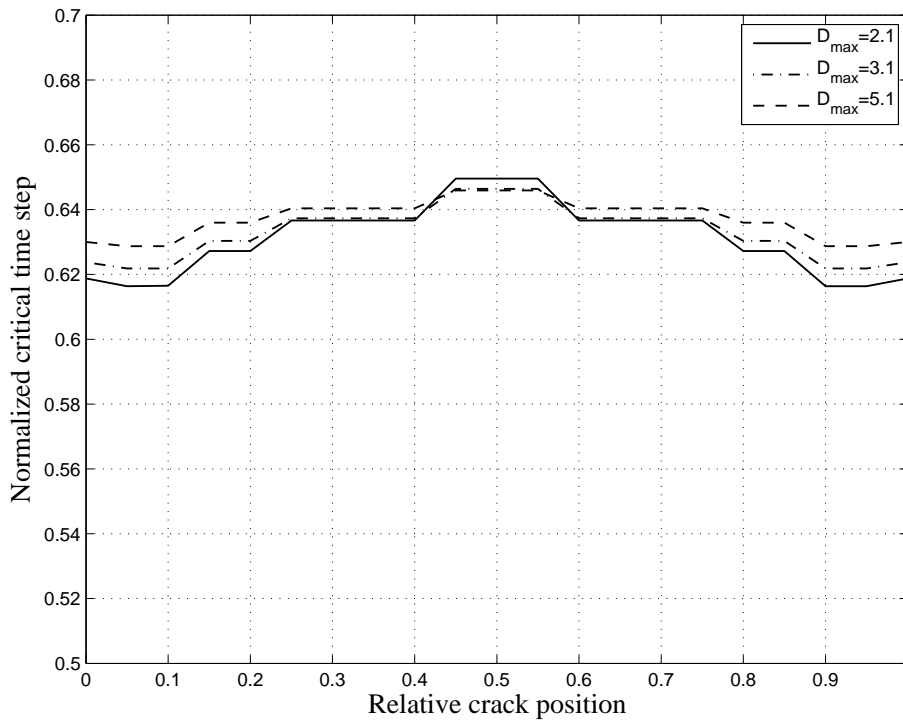Figure 7: Critical time step versus the crack position for mass lumping strategy 1 (MLS1) in 1D

Figure 8: Normalized critical time step versus the crack position for mass lumping strategy 1 (MLS1) in 2D
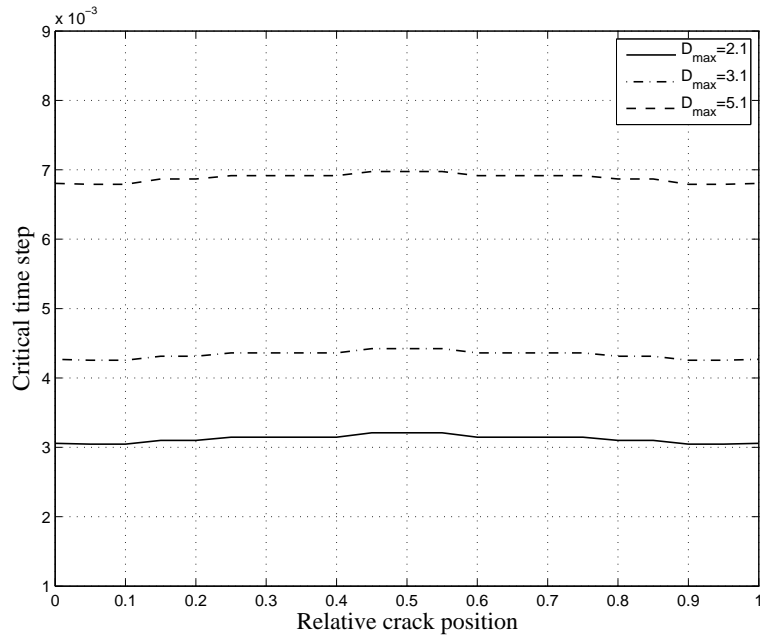
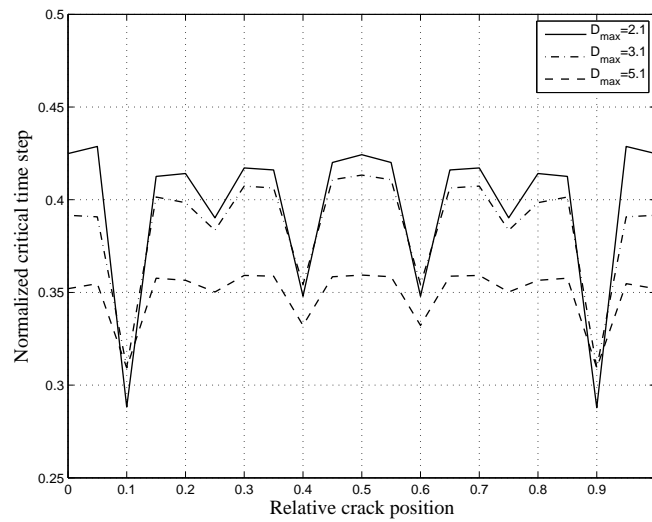Figure 9: Critical time step versus the crack position for mass lumping strategy 1 (MLS1) in 2D

Figure 10: Normalized Critical time step versus the crack position for mass lumping strategy 1 (MLS1) in 2D with tip enrichment
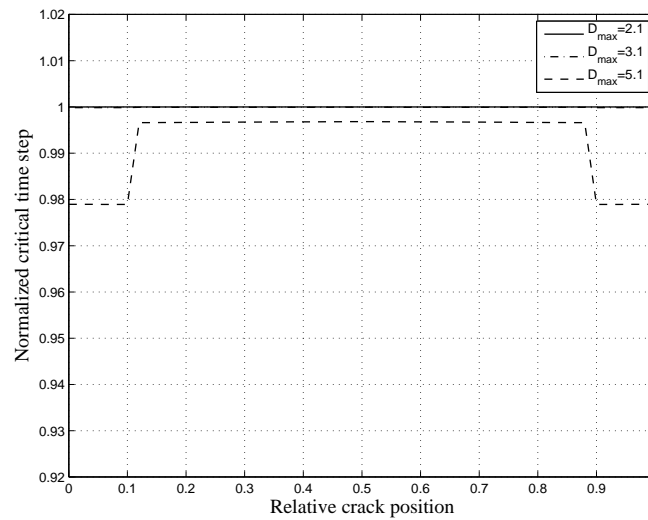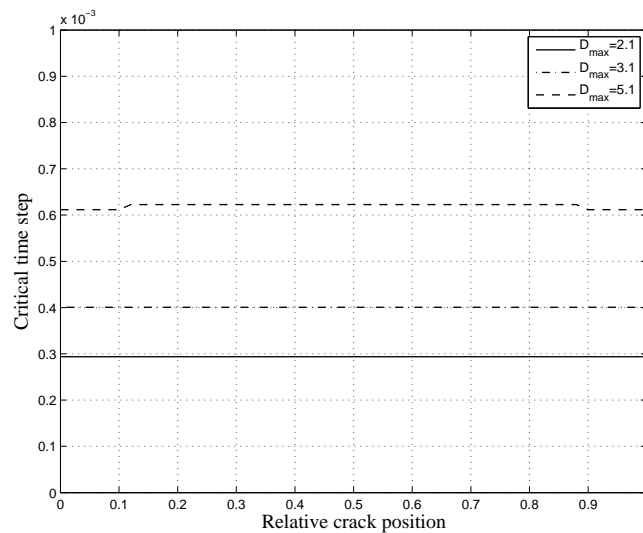
Figure 11: Normalized critical time step versus the crack position for mass lumping strategy 2 (MLS2) in 1D

Figure 12: Critical time step versus the crack position for mass lumping strategy 2 (MLS2) in 2D without tip enrichment

critical time step in MLS2 drops to 80% of Δt_{con} the MLS1 allows only 30% of Δt_{con}. We attribute these difference to the different mass values. While MLS1 conserves the mass of the whole system which implies smaller mass for some degrees of freedom which leads to smaller time step, the MLS2 increases the mass or in other words: $\sum_{I=1}^{N_{total}} M_{II}^{MLS1} < \sum_{I=1}^{N_{total}} M_{II}^{MLS2}$. For a pure rigid body motion of two crack surfaces, with $\boldsymbol{u} = \boldsymbol{0}$, MLS2 seems more appropriate and MLS1 will produce too small time steps; however, when the kinetic is not conserved[1], MLS2 will provide a mass value that is too large.

Now, we will obtain an analytic expression for the critical time step in the former case.

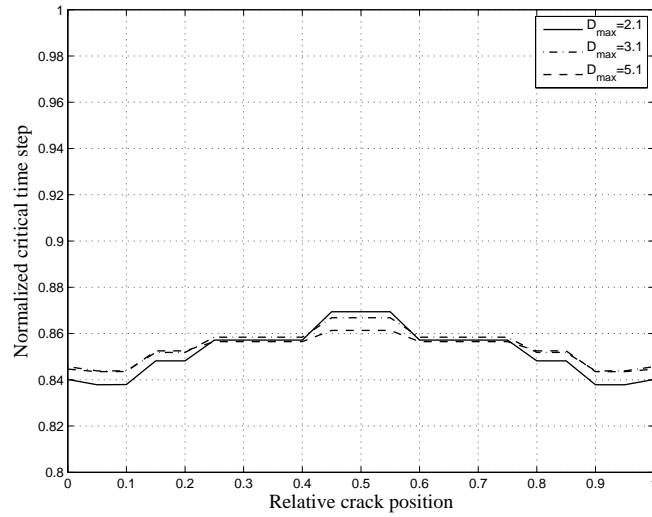[1]This will not be the case for generic problems.

Figure 13: Normalized Critical time step versus the crack position for mass lumping strategy 2 (MLS2) in 2D without tip enrichment
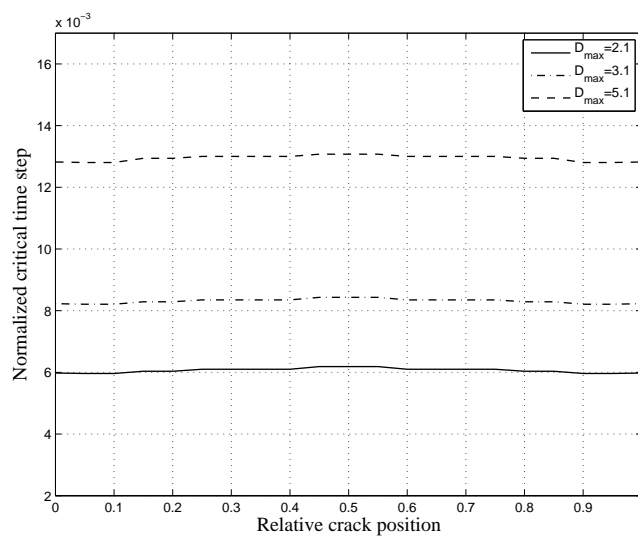

Figure 14: Critical time step versus the crack position for mass lumping strategy 2 (MLS2) in 2D without tip enrichment
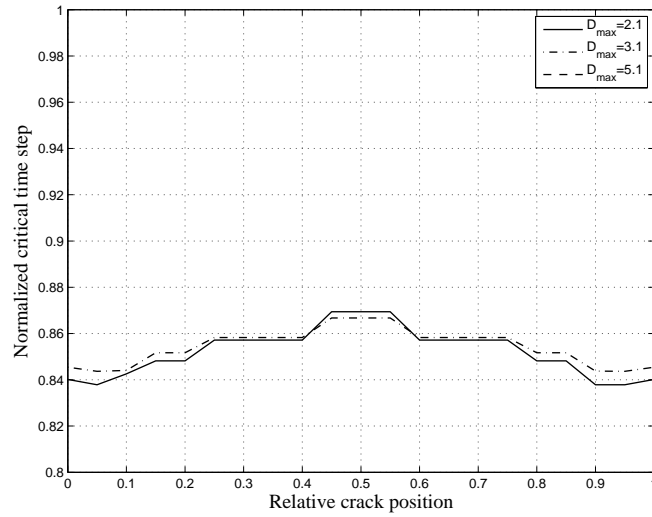
Figure 15: Normalized Critical time step versus the crack position for mass lumping strategy 2 (MLS2) in 2D with tip enrichment
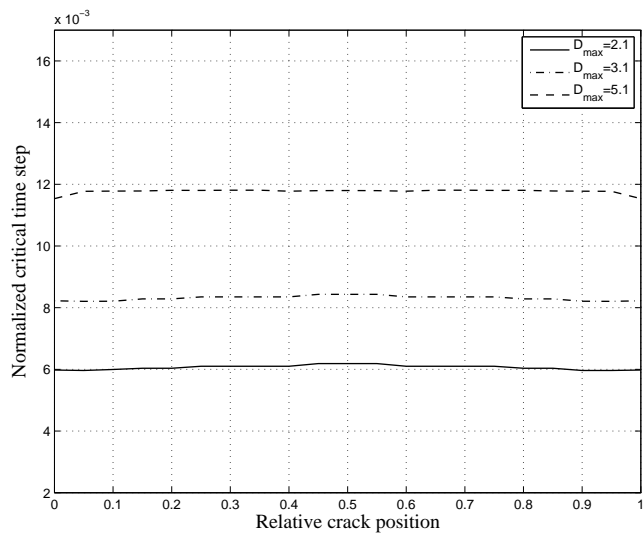

Figure 16: Critical time step versus the crack position for mass lumping strategy 2 (MLS2) in 2D with tip enrichment

4.3.3   Analytical Critical Time step Estimates

By using the fact that, for both mass lumping techniques studied here, the values of the critical time steps for the case with and without discontinuities are similar, we get some critical time step estimates for the latter case. Keep in mind that the second mass lumping technique reduces to the row-sum technique when no extra degrees of freedom are considered.

Consider a problem in one dimension. The domain is discretized in a finite set of nodes $[x_1, x_2, ..., x_N]$ that are uniformly spaced. The density is constant in all the domain. The intervals between the nodes define the integration cells.

Let us use a standard Element Free Galerkin method to solve the problem. The kernel functions are defined as cubic splines. The consistent mass and stiffness matrices in an integration cell are

$$M_{\text{cell}} = \varrho \int_{\Omega^c} \mathbf{\Phi}^T(x)\mathbf{\Phi}(x)d\Omega^c \tag{23}$$

and

$$\boldsymbol{K}_{\text{cell}} = \text{E} \int_{\Omega^c} \mathbf{\Phi}_x(x)\mathbf{\Phi}_x(x)d\Omega^c \tag{24}$$

where E is the Young's modulus,

$$\mathbf{\Phi} = \begin{bmatrix} \Phi_1(x) & \Phi_2(x) & ... & \Phi_n(x) \end{bmatrix} \tag{25}$$

are the shape functions, n the number of nodes that are different from zero in the integration cell and

$$\mathbf{\Phi}_{,x} = \begin{bmatrix} \Phi_{1,x}(x) & \Phi_{2,x}(x) & ... & \Phi_{n,x}(x) \end{bmatrix} \tag{26}$$

are the derivatives of the shape functions.

Solving the integrals defined in mass and stiffness matrices, we will obtain

$$M_{\text{cell}} = \rho\Delta x \begin{bmatrix} m_{11} & m_{12} & ... & m_{1n} \\ m_{21} & m_{22} & ... & m_{2n} \\ \vdots & \vdots & & \vdots \\ m_{n1} & m_{n2} & ... & m_{nn} \end{bmatrix} = \rho\Delta x M_{\text{dmax}} \tag{27}$$

and

$$\boldsymbol{K}_{\text{cell}} = \frac{\text{E}}{\Delta x} \begin{bmatrix} k_{11} & k_{12} & ... & k_{1n} \\ k_{21} & k_{22} & ... & k_{2n} \\ \vdots & \vdots & & \vdots \\ k_{n1} & k_{n2} & ... & k_{nn} \end{bmatrix} = \text{E}\frac{1}{\Delta x}\boldsymbol{K}_{\text{dmax}} \tag{28}$$

where Δx is the length of the integration cell and m_{ij} and k_{ij} depend on D_{max}. The matrices M_{dmax} and $\boldsymbol{K}_{\text{dmax}}$ are introduced for the sake of convenience in further derivations.

Now, we need to solve the generalized eigenvalue problem, focusing on finding the largest one. This eigenvalue is necessary to obtain an expression for the critical time step, as said before. With this aim in mind, we can show that

$$\lambda\left(M_{\text{cell}}, \boldsymbol{K}_{\text{cell}}\right) = \frac{\text{E}}{\rho\Delta x^2}\lambda\left(M_{\text{dmax}}, \boldsymbol{K}_{\text{dmax}}\right) \tag{29}$$

where λ is a generalized eigenvalue. The above expression is valid for both the consistent and the lumped mass matrices

For finding an estimate for the critical time step, valid for various values of the parameters involved, we will solve the eigenvalue problem for different values of D_{max} and then obtain an analytic expression by fitting techniques.

In Belytschko et al. (2000a) the largest eigenvalue obtained for the row-sum technique for the same one dimensional problem is

$$\lambda = \alpha \frac{E}{\varrho \Delta x^2 D_{max}^2} \tag{30}$$

where $\alpha = 13.30$. As shown in Belytschko et al. (2000a) this result can be generalized for two dimensional problems. We will adopt the form of this expression in order to perform the above mentioned fitting. With our framework, for the same mass lumping strategy we get $\alpha = 12.46$.

However, the expression obtained for λ with the first mass lumping is not very sharp. In practice, the critical time step estimates obtained seem to be excessively large. For these reasons, we propose an alternative that allows to obtain better estimations for λ.

In general, in the mass matrix integration cell there exist very small contributions of some nodes compared with other nodes. This effect enlarges the value of λ. However, in the global system, these big differences between the nodal contributions are not observed. Moreover, in practice, it seems that these small contributions spuriously decrease the critical time step estimation with respect to the real critical time step of the the global system.

We propose the following heuristic solution. Let us denote the length of the shape function support as s, and consider a local coordinate whose origin coincides with the initial point of the cell. In order to avoid small contributions, we will only consider the support of any shape function from $0.25s$ to $0.75s$. In Fig. 17, the dotted line shows the values that are excluded from the shape function. Also, we will only use even values for the parameter D_{max}. It is easy to see that this avoids very little contribution of some nodes in mass matrix.

As an example, see Fig. 18. We have an arbitrary integration cell defined between the nodes x_i and x_{i+1}. The value of D_{max} is equal to 4. The dotted line shows the values of the nodal shape functions that we exclude. That is, we are not considering the contribution of the shape functions associated with nodes x_{i-3}, x_{i-2}, x_{i+3} and x_{i+4}. Notice that these contributions are the smallest in the integration cell considered.

Finally, solving the eigenvalue problem for different even values of D_{max}, we obtain $\alpha = 7.1$ in Eq. (30) for the row-sum technique (relevant for mass lumping 2) and $\alpha = 10$ for the first mass lumping technique.

5 CONCLUSION

Some contributions to the analysis of the critical time step for partition of unity enriched meshfree methods in explicit dynamics for one-dimensional and two-dimensional problems were presented. Only uniformly distributed points were considered. The reader interested in more general examples is referred to Talebi et al. (2010). The enriched EFG method was studied, but the approach can be extended to other meshfree methods. We limited our studies to problems involving material failure with step enrichment. In a first step, we analyzed the critical time step for different positions of the crack when a consistent mass matrix is used. We found that in contrast to the extended finite element method, the critical time step does not drop to zero even for the worst case when the crack directly goes through a node. We attribute this effect to the overlapping meshfree shape functions. We observe that the critical time step increases when the domain of influence is increased which is in good agreement to results obtained e.g. in Belytschko et al. (2000a).
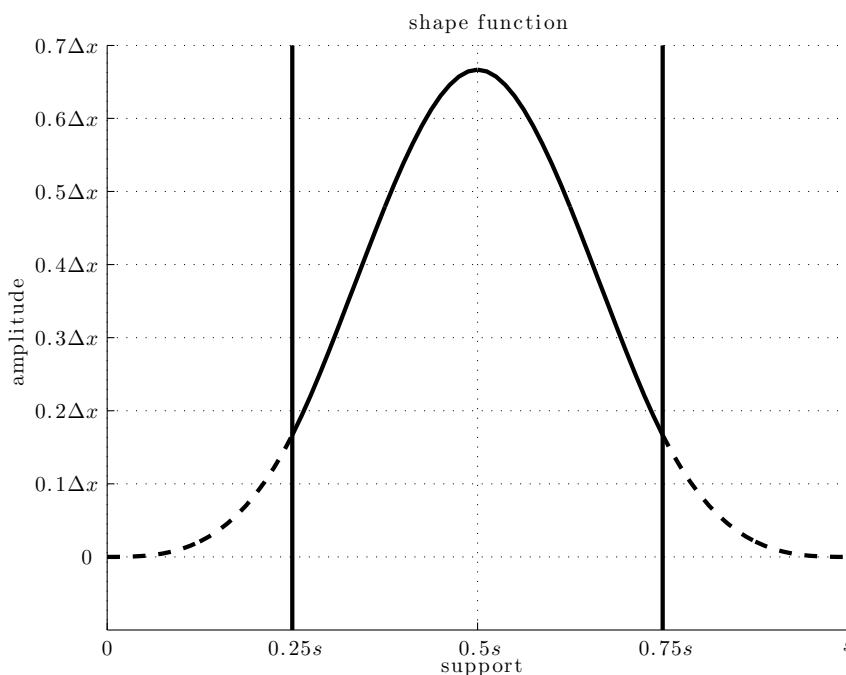
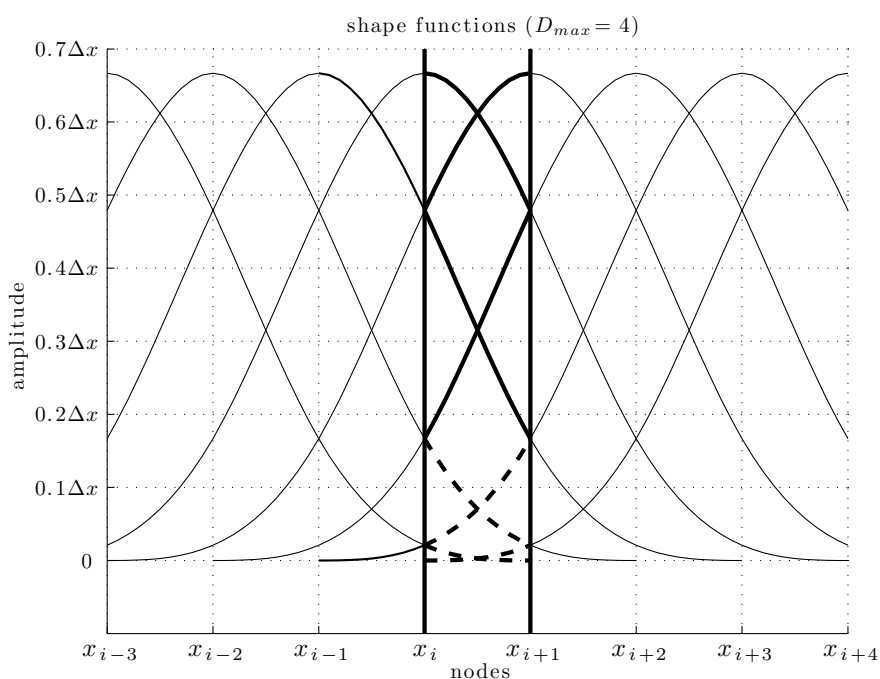Figure 17: Shape funtion. The dotted line are the values of the function that are not consider

Figure 18: Nodal shape functions in an integration cell. This cell is defined in the interval between the node x_i and the node x_{i+1}. The dotted line indicates the values of the shape functions that are not considered.

Afterwards, we proposed two ways of obtaining a diagonalized mass matrix for the enriched EFG method. The first idea is based on an approach from Hinton et al. (1976) and guarantees conservation of mass of the entire system. The second idea uses the concept of preserving the

continuum kinetic energy value after discretizacion, as presented by Menouillard et al. (2008) in the context of the extended finite element method. For the first method, the critical time step drops to a value of around 30-45% of the critical time step without enrichment. For the second method, the worst case scenario[1], gives a critical time step of around 84% of the critical time without any enrichment. We attribute these difference to a conceptual increase in the mass for the second approach. The diagonalized mass values might lie somewhere in between these two approaches.

Based on the assumption that the critical time step of the enriched formulation is of the order of the usual formulation, we analytically derived critical time step estimates that can be used for practical applications.

REFERENCES

Babuška I. and Melenk J.M. The partition of unity method. 40(4):727–758, 1997.

Belytschko T. and Black T. Elastic crack growth in finite elements with minimal remeshing. *International Journal for Numerical Methods in Engineering*, 45(5):601–620, 1999.

Belytschko T., Chen H., Xu J., and Zi G. Dynamic crack propagation based on loss of hyperbolicity and a new discontinuous enrichment. *International Journal for Numerical Methods in Engineering*, 58(12):1873–1905, 2003.

Belytschko T., Guo Y., Liu W., and Xiao S. A unified stability analysis of meshfree particle methods. *International Journal for Numerical Methods in Engineering*, 48:1359–1400, 2000a.

Belytschko T., Liu W.K., and Moran B. *Nonlinear Finite Elements for Continua and Structures*. John Wiley and Sons, 2000b.

Belytschko T., Lu Y.Y., and Gu L. Element free galerkin methods. *Int. J. Numer. Methods Eng.*, 37(2):229–256, 1994.

Chen J. and Wang H. A stabilized conforming nodal integration for galerkin meshfree-methods. *International Journal for Numerical Methods in Engineering*, 50:435–466, 2000.

Dolbow J., Moes N., and Belytschko T. Discontinuous enrichment in finite elements with a partition of unity method. *Finite Element Analysis and Design*, 36(3):235–260, 2000.

Fernandez-Mendez S. and Huerta A. Imposing essential boundary conditions in mesh-free methods. *Comput. Methods Appl. Mech. Eng.*, 2004. ISSN 0029-599X. Accepted for publication.

Flanagan DP. B.T. Eigenvalues and stable time steps for the uniform strain hexahedran and quadrilateral. *Journal of Applied Mechanics*, 51:35–40, 1981.

Hinton E., Rock T., and Zienkiewicz O. A note on mass lumping and related processes in finite element method. *Earthquake Engineering and Structural Dynamics*, pages 245–249, 1976.

Hughes T. *The Finite Element Method: Linear Static and Dynamic Finite Element Analysis,*. Dover Publications, New York, 1987.

Li S. and Liu W. Numerical simulations of strain localization in inelastic solids using mesh-free methods. *International Journal for Numerical Methods in Engineering*, 48(13):1285–1309, 2000.

M. A. Puso J. S. Chen E.Z.W.E. Meshfree and finite element nodal integration methods. *International Journal for Numerical Methods in Engineering*, 74:416–446, 2008.

Menouillard T., Rethore J., Moes N., Combescure A., and Bung H. Efficient explicit time stepping for the extended finite element method. *International Journal for Numerical Methods*

---

[1]A crack passes through a node

in Engineering, 68:931–938, 2006.

Menouillard T., Rethore J., Moes N., Combescure M., and Bung H. Mass lumping strategies for x-fem explicit dynamics: Application to crack propagation. *International Journal for Numerical Methods in Engineering*, 74(3):447–474, 2008.

Moes N., Dolbow J., and Belytschko T. A finite element method for crack growth without remeshing. *International Journal for Numerical Methods in Engineering*, 46(1):133–150, 1999.

Rabczuk T. and Belytschko T. Cracking particles: A simplified meshfree method for arbitrary evolving cracks. *International Journal for Numerical Methods in Engineering*, 61(13):2316–2343, 2004.

Rabczuk T. and Belytschko T. Application of meshfree particle methods to static fracture of reinforced concrete structures. *International Journal of Fracture*, 137(1-4):19–49, 2006.

Rabczuk T., Bordas S., and Zi G. A three dimensional meshfree method for static and dynamic multiple crack nucleation/propagation with crack path continuity. *Computational Mechanics*, 40(3):473–495, 2007.

Rabczuk T. and Zi G. A meshfree method based on the local partition of unity for cohesive cracks. *Computational Mechanics*, 39(6):743–760, 2007.

T. Elguedj A. Gravouil H.M. An explicit dynamics extended finite element method. part 1: Mass lumping for arbitrary enrichment functions. *Computer Methods in Applied Mechanics and Engineering*, 198(30-32):2297–2317, 2009.

Talebi H., Samaniego C., Samaniego E., and Rabczuk T. On the stability of explicit partition of unity enriched meshfree methods. *Submitted for publication to International Journal for Numerical Methods in Engineering*, 2010.

Ventura G., Xu J., and Belytschko T. A vector level set method and new discontinuity approximations for crack growth by efg. *International Journal for Numerical Methods in Engineering*, 54(6):923–944, 2002.

Wriggers P. *Nonlinear Finite Element Methods*. Springer, 2008.